Progress In Electromagnetics Research C, Vol. 48, 111–123, 2014

A Novel Planar Structure for Implementing Power Divider or Balun with Variable Power Division

Weiwei Zhang[1, *], Yuanan Liu[1], Yongle Wu[1, 2], Junyu Shen[1], Shulan Li[1], Cuiping Yu[1], and Jinchun Gao[1]

Abstract—A simple and analytical design methodology for a novel planar four-port structure to implement power divider (PD) or balun with variable power division is proposed in this paper. It consists of two different 3 dB branch-line couplers and one coupled-line phase shifter whose length can be changed to implement variable power division. Different from the previous designs, the power divider and balun with variable power division can be realized in only one circuit by changing the electrical length θ_0 of the coupled line when the impedance ratio g is selected. According to the $ABCD$ parameters and linear algebra calculation, closed-form mathematical equations for the circuit electrical values and scattering parameters can be obtained. A prototype with this proposed circuit, operating at 2 GHz, has been designed and fabricated using microstrip technology. Good agreements between the calculated and measured results verify our design.

1. INTRODUCTION

Power divider (PD) is widely applied in the RF/microwave power amplifiers, the front end of the antennas, many kinds of test equipment and other modern microwave or millimeter-wave engineering, because of its convenient design and good performance. It can be matched at all ports and provide perfect isolation between output ports [1, 2]. This kind of PD can be realized with coaxial cable, microstrip line, and coplanar waveguide and so on. Different from the traditional equal PD, the unequal PD, which is available in the form of lumped-element or distributed designs, has been used with strict restrictions in design and fabrication because it requires a microstrip line with very high characteristic impedance. For example, a $N : 1$ ($N \geqslant 4$) Wilkinson PD requires more than 130 Ω microstrip line which cannot be realized by the conventional microstrip structure [3]. In practice, the characteristic impedance of a realizable microstrip has its limitation which is usually lower than 130 Ω. Therefore, it is hard to realize $N : 1$ ($N \geqslant 4$) power ratio by using the conventional microstrip Wilkinson PD structure.

To overcome this shortcoming, some new types of unequal Wilkinson PDs with high power division ratio were proposed. The methods are mainly summarized as follows: the microstrip line with Defected Ground Structure (DGS) patterns [4–8], double-sided parallel-strip lines (DSPSL) [9–11], composite right left-handed transmission lines (CRLH-TLs) [12–14], a two-port filtering structure connected to a circulator [15, 16] and other methods [17–19].

The microstrip line with DGS patterns in the ground plane was used to increase the characteristic impedance by etching off a certain defected pattern from ground plane. A 4 : 1 unequal Wilkinson PD, which uses the microstrip line with the DGS, was designed in [7]. An unequal $1 : N$ Wilkinson PD with variable power dividing ratio, which is composed of the conventional Wilkinson PD structure, rectangular-shaped DGS, was designed in [8]. However, the design procedure is relatively complex and

Received 15 December 2013, Accepted 26 February 2014, Scheduled 18 March 2014

* Corresponding author: Weiwei Zhang (clarence.zhang11@gmail.com).

[1] Beijing Key Laboratory of Work Safety Intelligent Monitoring, Beijing University of Posts and Telecommunications, Beijing, China.

[2] The State Key Laboratory of Millimeter Waves, Southeast University, Nanjing 210096, China.

there is no general analytical methods. Moreover, DSPSL [9–11] can realize high impedance by offsetting the top and bottom strips, which cannot be achieved by using other conventional transmission lines such as microstrip line due to its fabrication limitation. For example, a novel 5 : 1 unequal Wilkinson PD using the offset DSPSL was proposed in [10]. CRLH-TLs [12–14], which are implemented by loading a conventional RHTL with series capacitance and shunt inductance, are artificial structures. In addition, the ground layer is needed in both DGS and DSPSL, which will affect other layers in multi-layer boards. CRLH-TLs are designed to exhibit some special properties that are not available when using conventional transmission lines. In [12], a dual-band equal 1 : 4 series PD and an unequal divider with a power dividing ratio of 1 : 2 : 2 : 1 were designed based on the CRLH-TLs and nonradiating CRLH-TLs. [15, 16] provided a novel type of power divider, featuring arbitrary power ratio and arbitrary ripple level. Other methods [17–19], such as using shunt stubs [17], using coupled lines with two shorts [18], using a microstrip line with a periodic shunt open stub to achieve low-impedance lines [19], were also adopted to design unequal PD with high power-dividing ratio.

In this paper, a novel four-port circuit structure for implementing PD or balun with variable power division, which is suitable for microstrip printed circuit board (PCB) realization, is proposed. The difference from the previous unequal PD or balun is that the circuit consists of two different 3 dB branch-line couplers and one phase shifter whose length can be adjusted to implement variable power division when the impedance ratio g is seclected. This proposed four-port circuit structure is expected to exhibit several advantages including: 1) **arbitrary power division ratio**; 2) **easy adjustment only by changing the length of the coupled line when g is selected**; 3) **inherent impedance transforming function;** 4) ideal all ports matching; 5) perfect isolation between the two output ports; 6) analytical design equations for circuit electrical parameters and scattering parameters; 7) planar structure and easy realization in common microstrip technology. In Section 2, the proposed circuit structure and the design theory are derived by using the $ABCD$ parameters and the linear algebra calculation. The scattering parameters are given at last. For discussing the influence of the circuit parameters, the electrical length θ_0 and the impedance ratio g of the coupled line are discussed in Section 3. The experimental microstrip circuit prototype has been fabricated and measured. The consistency between calculated and measured results validates this proposed circuit structure in Section 4. A conclusion is presented in Section 5.

2. THE PROPOSED CIRCUIT STRUCTURE AND DESIGN THEORY

The circuit configuration of the proposed four-port circuit structure is shown in Figure 1. It is an asymmetric circuit terminated by equal real impedance R_s for both the port 1 (input port) and port 4 (isolation port) on the left side. This circuit has the same impedance R_L in ports 2 and 3 (output port) on the right side. This circuit essentially includes two different 3 dB branch-line couplers and one phase shifter. It can be easily seen that this circuit has internal impedance transforming performance. To analyze this circuit clearly, three parts are divided as follows.

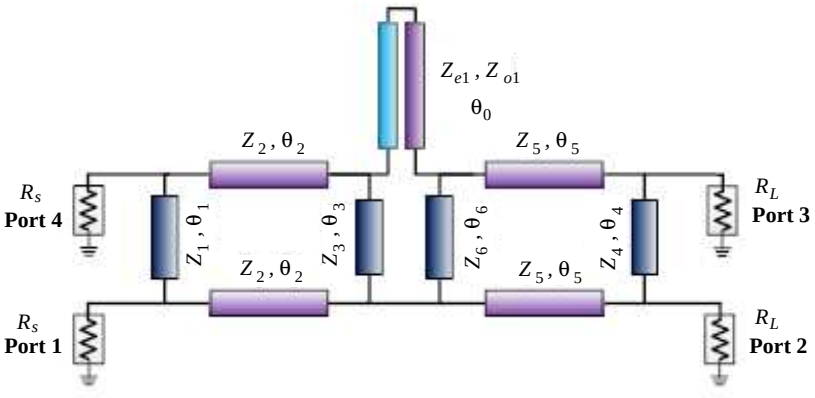

Figure 1. The circuit configuration of the proposed structure.

2.1. The 3 dB Branch-line Coupler

Figure 2 shows the schematic of the traditional 3 dB branch-line coupler with the equal real impedance R_1 at the left side and R_2 at the right side. Moreover, left (right) branch has the characteristic impedance of Z_1 (Z_3) and electrical lengths of θ_1 (θ_3). Meanwhile, the characteristic impedance of the transmission line located at the center place is Z_2, and the corresponding electrical length is θ_2. In order to simplify the analysis process, $\theta_1 = \theta_2 = \theta_3 = 90^\circ$ are chosen. In fact, the 3 dB branch-line coupler has the same circuit structure with [20] and has the same analysis methods. Here just lists the analysis results:

$$Z_1 = R_1, \tag{1a}$$

$$Z_2 = \sqrt{\frac{R_1 R_2}{2}}, \tag{1b}$$

$$Z_3 = R_2. \tag{1c}$$

The scattering parameters of the 3 dB branch-line coupler are:

$$\begin{bmatrix} b_1 \\ b_2 \\ b_3 \\ b_4 \end{bmatrix} = \frac{-1}{\sqrt{2}} \begin{bmatrix} 0 & j & 1 & 0 \\ j & 0 & 0 & 1 \\ 1 & 0 & 0 & j \\ 0 & 1 & j & 0 \end{bmatrix} \begin{bmatrix} a_1 \\ a_2 \\ a_3 \\ a_4 \end{bmatrix}, \tag{2}$$

where a_i and b_i denote the incident and reflected wave of the port i, ($i = 1$, 2, 3, and 4).

2.2. The Coupled-line Phase Shifter

The phase shifter in Figure 3 is composed of the parallel-coupled lines with the same electrical lengths which are connected at one end [21]. The analysis have been given in [21] and here just list some results.

$$Z_{e1} Z_{o1} = Z_0^2. \tag{3}$$

The scattering parameters are:

$$S_{11} = S_{22} = 0, \tag{4a}$$

$$S_{12} = S_{21} = \frac{Z_{e1} \cot\theta_0 + Z_{o1} \tan\theta_0}{Z_{e1} \cot\theta_0 - Z_{o1} \tan\theta_0 + j2Z_0} = e^{j\psi}, \tag{4b}$$

where the phase shifter ψ is defined by:

$$\cos\psi = \frac{g - \tan^2\theta_0}{g + \tan^2\theta_0}. \quad \left(g = \frac{Z_{e1}}{Z_{o1}}\right) \tag{5}$$

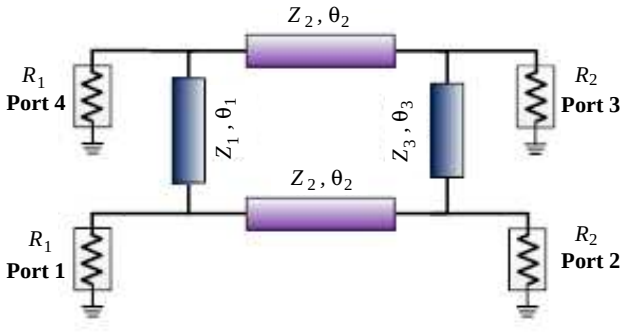

Figure 2. The circuit configuration of the 3 dB branch-line coupler.

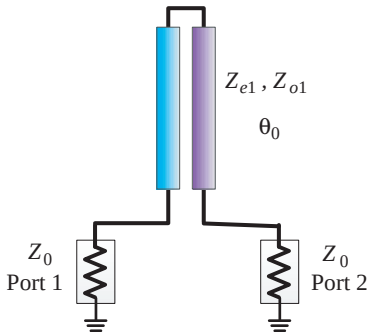

Figure 3. The circuit configuration of the coupled-line phase shifter.

2.3. Analysis of the Proposed Circuit Structure

In order to analyze the proposed circuit clearly, the corresponding diagram of this circuit is illustrated in Figure 4.

According to Equation (2), the scattering parameters of the 3 dB branch-line couplers 1 and 2 can be obtained as follows:

$$\begin{bmatrix} b_1 \\ b_2' \\ b_3' \\ b_4 \end{bmatrix} = \frac{-1}{\sqrt{2}} \begin{bmatrix} 0 & j & 1 & 0 \\ j & 0 & 0 & 1 \\ 1 & 0 & 0 & j \\ 0 & 1 & j & 0 \end{bmatrix} \begin{bmatrix} a_1 \\ a_2' \\ a_3' \\ a_4 \end{bmatrix}, \tag{6a}$$

$$\begin{bmatrix} b_1' \\ b_2 \\ b_3 \\ b_4' \end{bmatrix} = \frac{-1}{\sqrt{2}} \begin{bmatrix} 0 & j & 1 & 0 \\ j & 0 & 0 & 1 \\ 1 & 0 & 0 & j \\ 0 & 1 & j & 0 \end{bmatrix} \begin{bmatrix} a_1' \\ a_2 \\ a_3 \\ a_4' \end{bmatrix}. \tag{6b}$$

According to Equation (4), the relationships between the incident and reflected wave are:

$$a_1' = b_2', \tag{7a}$$

$$a_2' = b_1', \tag{7b}$$

$$a_3' = b_4' e^{j\psi}, \tag{7c}$$

$$a_4' = b_3' e^{j\psi}. \tag{7d}$$

After some linear computation, the final scattering parameters at the operating frequency can be achieved by solving the Equations (6), (7)

$$\begin{bmatrix} b_1 \\ b_2 \\ b_3 \\ b_4 \end{bmatrix} = \frac{1}{2} \begin{bmatrix} 0 & (e^{j\psi}-1) & j(e^{j\psi}+1) & 0 \\ (e^{j\psi}-1) & 0 & 0 & j(e^{j\psi}+1) \\ j(e^{j\psi}+1) & 0 & 0 & (1-e^{j\psi}) \\ 0 & j(e^{j\psi}+1) & (1-e^{j\psi}) & 0 \end{bmatrix} \begin{bmatrix} a_1 \\ a_2 \\ a_3 \\ a_4 \end{bmatrix}. \tag{8}$$

It can be clearly seen that the equation $|S_{21}|^2 + |S_{31}|^2 = 1$ indicates the energy conservation. The power division ratio $K = |S_{21}|^2/|S_{31}|^2$ can also be obtained from the Equation (8):

$$K = \frac{|S_{21}|^2}{|S_{31}|^2} = \frac{1-\cos\psi}{1+\cos\psi} = \frac{\tan^2\theta_0}{g}. \tag{9}$$

From Equation (9), it can be observed that the power division ratio K, which can be adjusted by changing the electrical length θ_0 and the impedance ratio g of the coupled line, can be equal to any real numbers at the operating frequency, indicating that the **arbitrary power division ratio** can be obtained using this proposed circuit structure. The arbitrary power division ratio K will be discussed in Section 3.1 specifically.

In addition, the following can be obtained from the Equations (8), and (9):

$$S_{21} = -\sqrt{K} S_{31} \quad (0^\circ < \theta_0 < 90^\circ), \tag{10a}$$

$$S_{21} = \sqrt{K} S_{31} \quad (90^\circ < \theta_0 < 180^\circ). \tag{10b}$$

Equation (10) is the theoretical support of implementing PD or balun with variable power division by adjusting the electrical length θ_0 and impedance ratio g of the coupled line.

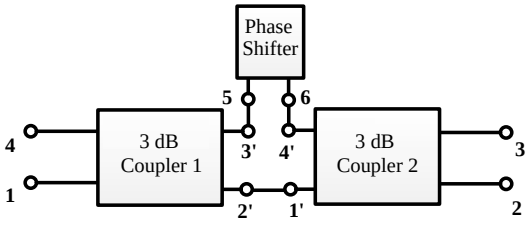

Figure 4. The diagram of the proposed structure.

3. ANALYSIS OF THE CIRCUIT ELECTRICAL PARAMETERS

Based on the previous theoretical investigation, the closed solutions of the proposed circuit and the scattering parameters are obtained. For a given set of circuit values (R_s, R_L, g, and θ_0), other unknown values can be easily calculated. The next step is to discuss the effect of electrical length θ_0 and the impedance ratio g of the coupled line to the power division ratio K.

3.1. The Discussion about the Electrical Length θ_0 and Impedance Ratio g

The advantage of this proposed circuit structure is that it can realize the PD or balun with variable power division K in only one circuit by adjusting the electrical length θ_0 and the impedance ratio g of the coupled line. Figure 5 illustrates the phase difference between the output ports 2 and 3, the scattering parameters of the output ports, the power division $K = |S_{21}|^2/|S_{31}|^2$ when θ_0 varies from 0° to 180° and the impedance ratio g is equal to 1.1, 1.4, and 1.7, respectively. When θ_0 varies from 0° to 90°, the phase difference between port 2 and 3 are −180° which can be used to realize a balun. The power divider can be realized when θ_0 is between 90° and 180°. This conclusion can also be verified from the Equation (10).

Figure 5(c) illustrates the power division K can be arbitrary when the electrical length θ_0 varies from 0° to 180°. The value of g has a little effect on the scattering parameters and the power division. Moreover, the influence of g will be discussed in the Section 3.4.

Table 1 lists the special cases ($\theta_0 = 0°$, 90°, and 180°). It can be seen when the electrical length θ_0 is equal to 0° or 180°, all energies, which are from the port 1, are transferred to the port 3 totally

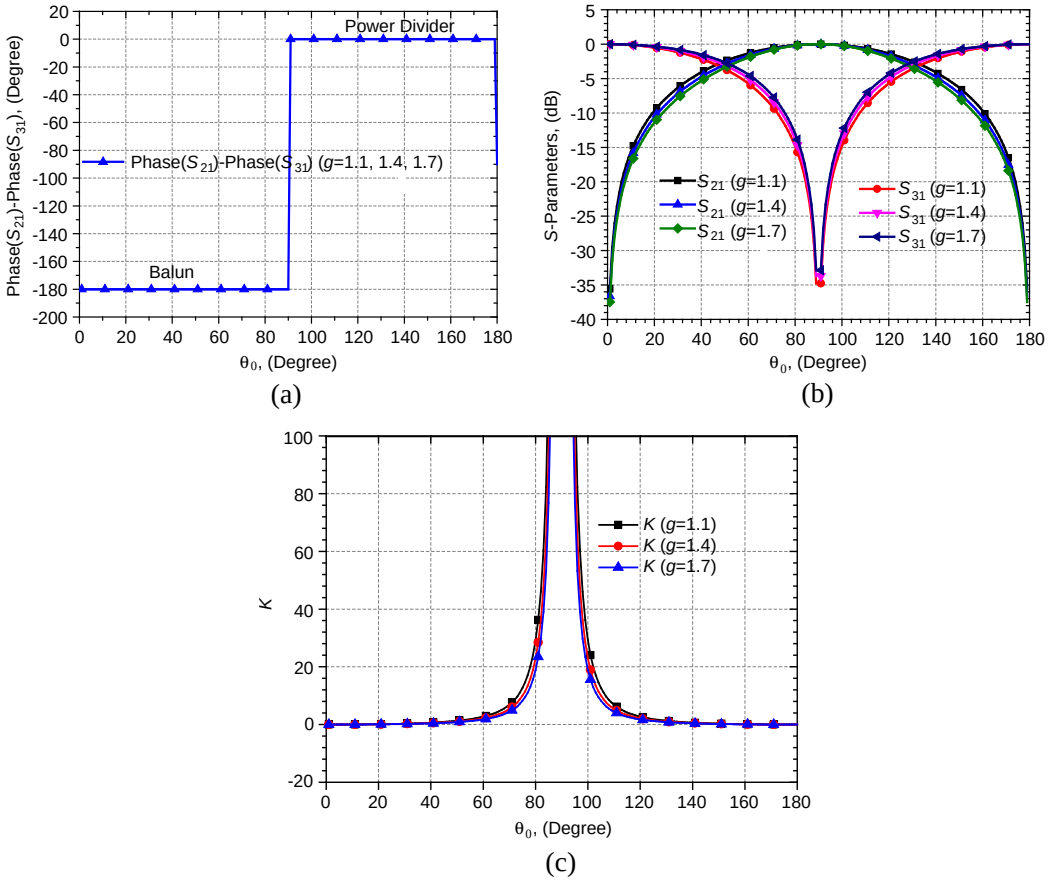

Figure 5. (a) The phase difference of the output ports vs θ_0. (b) The S-parameters of the output ports vs θ_0. (c) The power division K vs θ_0.

Table 1. The special cases of the proposed circuit structure.

θ_0 (°)	ψ (°)	S_{21}	S_{31}	$\angle S_{21} - \angle S_{31}$
0°	0°	0	j	−90°
90°	−180°	−1	0	−180°
180°	0°	0	j	−90°

with 90° phase shift. Note that the port 2 is not a throughout port and no energies are transferred to port 2 in this case. Similarly, all energies, which are from the port 1, are transferred to port 2 totally with −180° phase shift and no energies are transferred to port 3 when the electrical length θ_0 is equal to 90°.

3.2. The Research of the Balun Realization

From Section 3.1, the balun with variable power division can be realized when θ_0 is between 0° and 90° (0° and 90° are excluded). It is assumed that three examples 1, 2, and 3 operate at 2 GHz. The circuit parameters are $R_s = 60\,\Omega$, $R_L = 60\,\Omega$, $Z_1 = 60\,\Omega$, $Z_2 = 38.7298\,\Omega$, $Z_3 = 50\,\Omega$, $Z_4 = 80\,\Omega$, $Z_5 = 44.7214\,\Omega$, $Z_6 = 50\,\Omega$, $Z_{e1} = 52.4404\,\Omega$, $Z_{o1} = 47.6731\,\Omega$, and $g = 1.1$. The electrical lengths $\theta_0 = 30°$, 60°, and 80° of the coupled line are chosen as examples 1, 2, and 3 to show the property of the balun in Figure 6. Figure 6 shows the balun has the good port match $S_{11} = 0$, $S_{41} = 0$, the perfect isolation parameter $S_{23} = 0$ at the operating frequency. From Figure 6, the output scattering parameters and the power division K at the operating frequency in these three examples are concluded in Table 2.

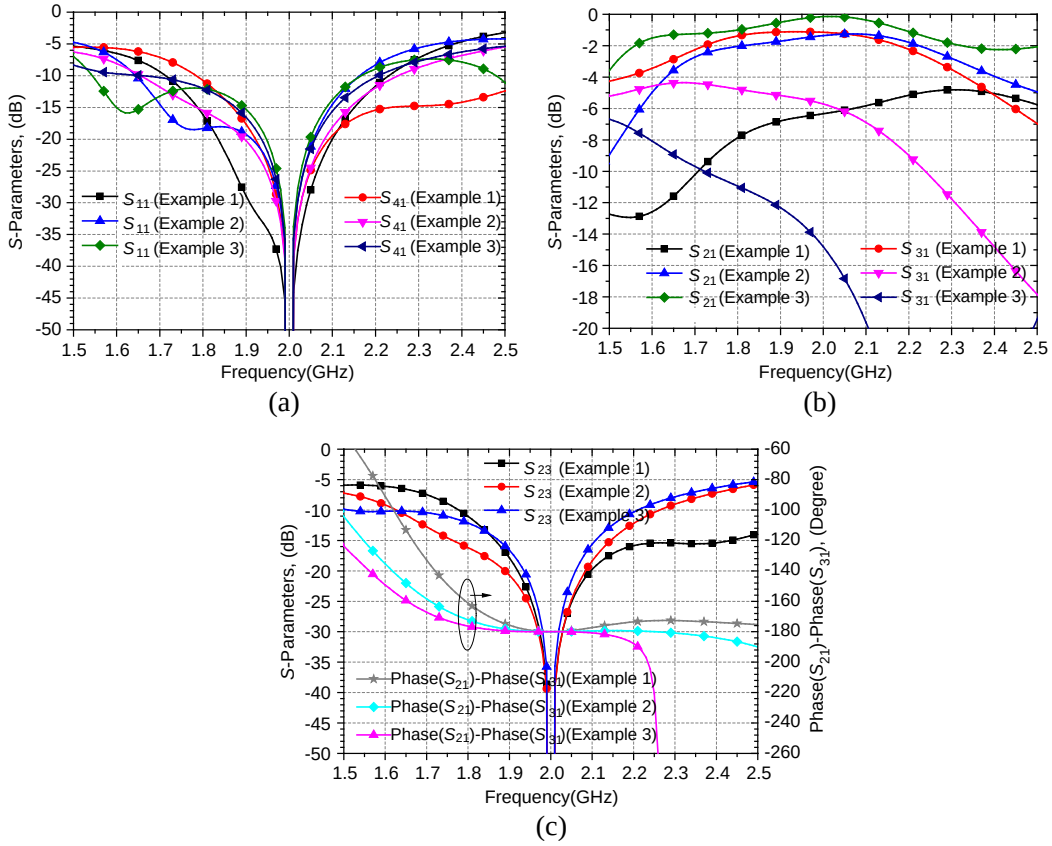

Figure 6. The scattering parameters of the proposed balun (a) S_{11}, and S_{41}. (b) S_{21}, and S_{31}. (c) S_{23} and the phase difference between the ports 2 and 3.

Table 2. The scattering parameters and power division at the operating frequency.

	θ_0 (°)	S_{21} (dB)	S_{31} (dB)	K	$\angle S_{21} - \angle S_{31}$ (°)
Example 1	30	−6.335	−1.15	0.3030	−180
Example 2	60	−1.357	−5.714	2.7273	−180
Example 3	80	−0.146	−14.806	29.2395	−180

From Table 2, when θ_0 is equal to 30°, 60°, and 80°, respectively, and the power division K is equal to 0.3030, 2.7273, and 29.2395 correspondingly, which indicates that the power division can be decided by the θ_0 when g is selected. The phase difference between the output port means that the circuit is a balun.

Note that the scattering parameters can be seen from Figure 5(b), and the power division K can be seen from Figure 5(c). The different power division K can be obtained by changing the electrical length θ_0 of the coupled line.

3.3. The Research of the PD Realization

From Section 3.1, the PD with variable power division can be realized when θ_0 is between 90° and 180° (90° and 180° are excluded). It is assumed that three examples 4, 5, and 6 operate at 2 GHz. The circuit parameters are $R_s = 60\,\Omega$, $R_L = 60\,\Omega$, $Z_1 = 60\,\Omega$, $Z_2 = 38.7298\,\Omega$, $Z_3 = 50\,\Omega$, $Z_4 = 80\,\Omega$, $Z_5 = 44.7214\,\Omega$, $Z_6 = 50\,\Omega$, $Z_{e1} = 52.4404\,\Omega$, $Z_{o1} = 47.6731\,\Omega$, and $g = 1.1$. The electrical lengths $\theta_0 = 110°$, 140°, and 170° of the coupled line are chosen as examples 4, 5, and 6 to show the property of the PD in Figure 7. Similar to the balun, the PD has the good port match $S_{11} = 0$, $S_{41} = 0$, and the

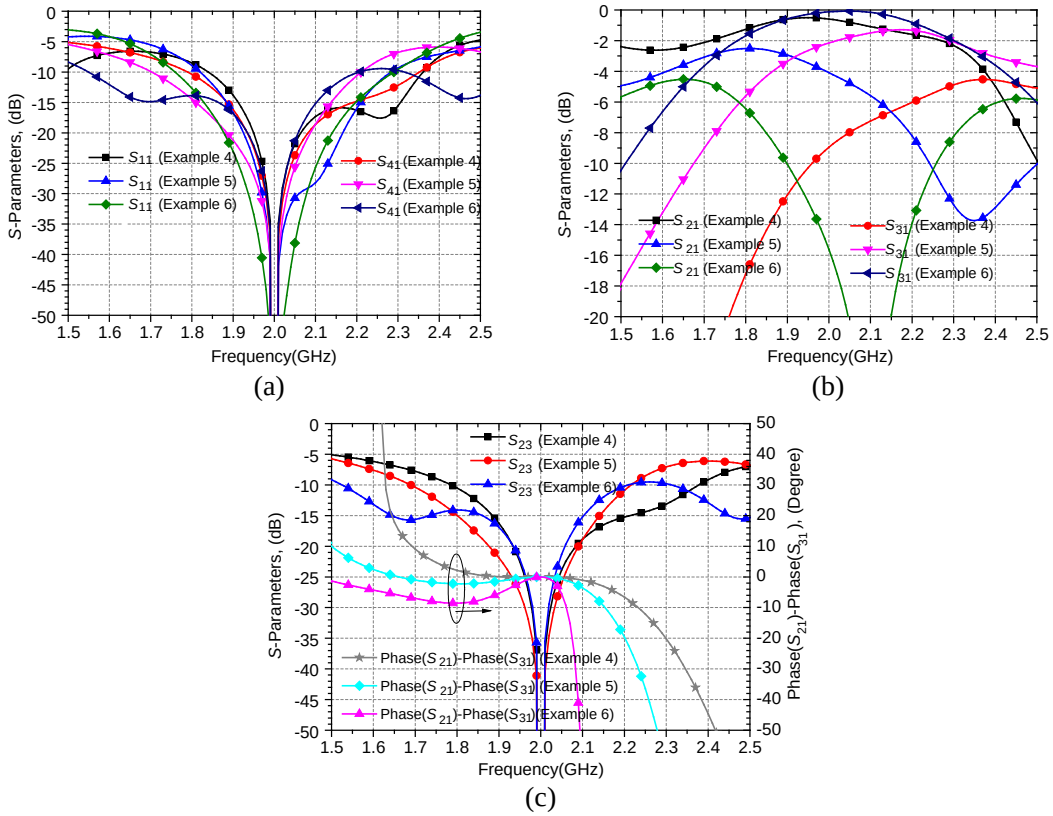

Figure 7. The Scattering parameters of the proposed PD (a) S_{11}, and S_{41}. (b) S_{21}, and S_{31}. (c) S_{23} and the phase difference between the ports 2 and 3.

Table 3. The scattering parameters and power division at the operating frequency.

	θ_0 (°)	S_{21} (dB)	S_{31} (dB)	K	$\angle S_{21} - \angle S_{31}$(°)
Example 4	110	−0.591	−8.956	6.8624	0
Example 5	140	−4.086	−2.149	0.6401	0
Example 6	170	−15.609	−0.121	0.0283	0

perfect isolation parameter $S_{23} = 0$ at the operating frequency. From Figure 7, the output scattering parameters and the power division in these three examples are concluded in Table 3.

From Table 3, when θ_0 is equal to 110°, 140°, and 70°, respectively, the power division K is equal to 6.8620, 0.6401, and 0.0283 correspondingly, which indicates that the power division can be decided by the θ_0 when g is selected. The phase difference between the output port means that the circuit is a power divider.

Note that the scattering parameters can be seen from Figure 5(b), and the power division K can be seen from Figure 5(c). The different power division K can be obtained by changing the electrical length θ_0 of the coupled line.

3.4. The Influence of the Impedance Ratio g of the Coupled Line

For observing the effects of the impedance ratio g of the coupled line, Table 4 lists the design parameters (Z_{e1}, Z_{o1}) of the three examples (7, 8, 9) with different impedance ratio g. It is assumed that these three examples operate at 2 GHz. Other parameters are $R_s = 60\,\Omega$, $R_L = 60\,\Omega$, $Z_1 = 60\,\Omega$, $Z_2 = 38.7298\,\Omega$,

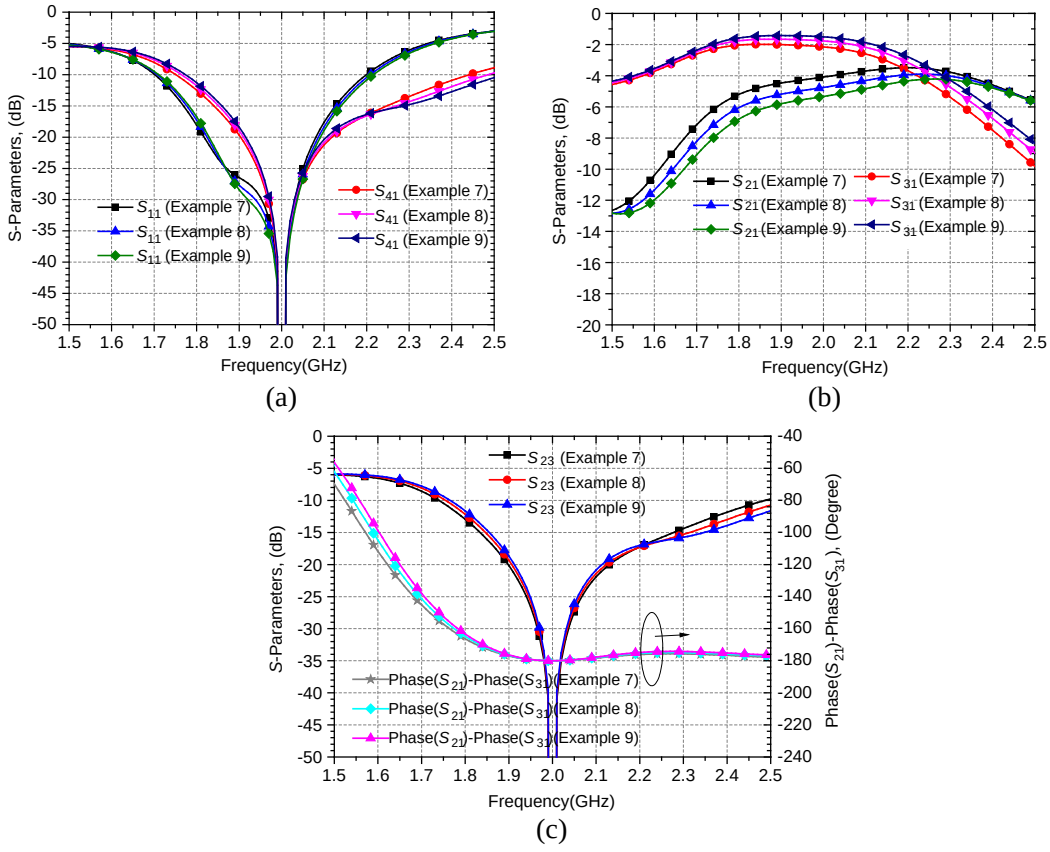

Figure 8. The scattering parameters of the proposed power divider (a) S_{11}, and S_{41}. (b) S_{21}, and S_{31}. (c) S_{23} and the phase difference between the ports 2 and 3.

Table 4. The design parameters of the examples 7, 8, 9 and the scattering parameters at the operating frequency.

	g	Z_{e1} (Ω)	Z_{o1} (Ω)	S_{21} (dB)	S_{31} (dB)	K
Example 7	1.1	52.4404	47.6731	−4.086	−2.149	0.1204
Example 8	1.4	59.1608	42.2577	−4.754	−1.769	0.0946
Example 9	1.7	65.1920	38.3482	−5.333	−1.505	0.0779

$Z_3 = 50\,\Omega$, $Z_4 = 80\,\Omega$, $Z_5 = 44.7214\,\Omega$, $Z_6 = 50\,\Omega$, $\theta_0 = 20°$. Figure 8 illustrates the calculated scattering parameters of this proposed circuit, which are based on lossless coupled-line model. From Table 4 and Figure 8, it can be observed that with the increase of the characteristic impedances, the power division change a little.

From Table 4, when g is equal to 1.1, 1.4, and 1.7, respectively, the power division K is equal to 0.1204, 0.0946, and 0.0779 correspondingly, indicating the alteration of g affects little to the power division and the scattering parameters. The g can be chosen to be 1.4 after taking the practical realization into consideration. Note that the scattering parameters can be seen from Figure 5(b) and the power division K can be seen from Figure 5(c).

4. EXAMPLES

The design theory and parameter analysis of this proposed circuit have been explained in Sections 2 and 3. To verify our proposed idea experimentally, an example with $\theta_0 = 40°$, $g = 1.4$ is designed, fabricated, and measured in this section. The F4B substrate with a relative dielectric constant of 2.65 and a thickness of 1 mm is used. According to the previous analysis, the following initial electrical parameters of the balun are calculated and summarized as follows: $R_s = 60\,\Omega$, $R_L = 80\,\Omega$, $Z_1 = 60\,\Omega$, $Z_2 = 38.7298\,\Omega$, $Z_3 = 50\,\Omega$, $Z_4 = 80\,\Omega$, $Z_5 = 44.7214\,\Omega$, $Z_6 = 50\,\Omega$, $Z_{e1} = 59.1608\,\Omega$, $Z_{o1} = 42.2577\,\Omega$, $g = 1.4$, $\theta_0 = 40°$. Note that the source and load impedance are not $50\,\Omega$ and in order to be measured by the Vector Network Analyzer easily, four transmission line transformers with the electrical length of 90° are adopted between each port and the circuit. The characteristic impedance Z_s ($54.7723\,\Omega$), which is between the input ports (1, 4) and the circuit, and Z_l ($63.2456\,\Omega$), which is between the output ports (2 and 3) and the circuit, are adopted to realize port impedance transformation to $50\,\Omega$.

In addition, the operating frequency of this example is 2 GHz. The above-layer circuit trace layout of the proposed circuit structure with defined dimension parameters is shown in Figure 9. Figure 10 illustrates the top view of the fabricated microstrip circuit. The physical circuit parameters are listed in Table 5. The method of putting elbows in Figure 9 is to reduce the coupling between the microstrip line Z_3 and Z_6.

The measured results are obtained by using Agilent N5230C network analyzer. The calculated and measured results are illustrated in Figure 11. Figure 11 shows the high isolation between the port 2 and port 3. The measured value of S_{41} are −17.59 dB at the operating frequency. The calculated values of

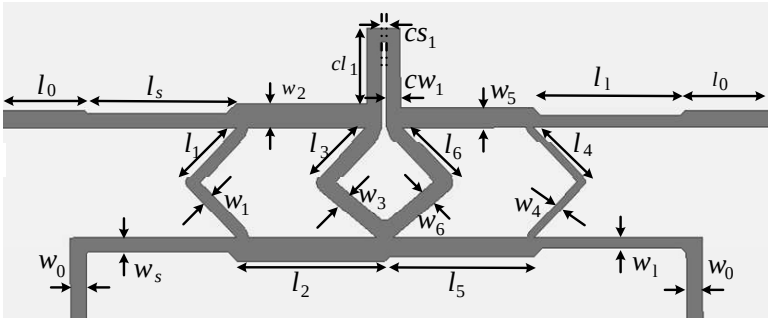

Figure 9. The physical definition of the proposed circuit structure.

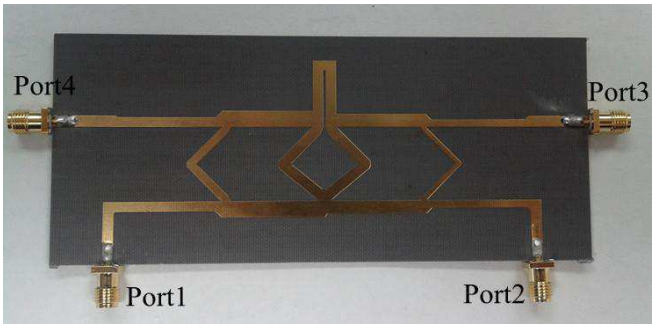

Figure 10. Top view of the fabricated microstrip circuit.

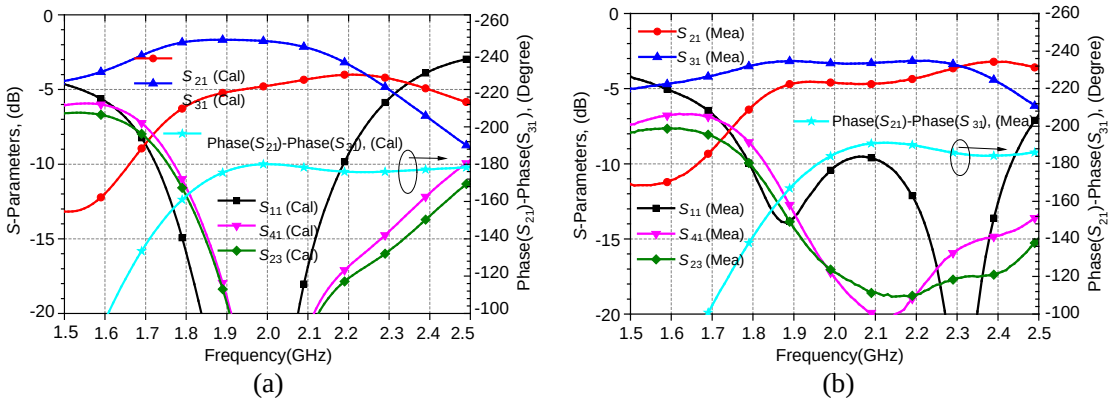

Figure 11. (a) The calculated scattering parameters of the circuit. (b) The measured scattering parameters of the circuit.

Table 5. The physical circuit parameters (unit: mm) of the example.

w_0	l_0	w_1	l_1	w_2	l_2	w_3	l_3	w_4	l_4	w_5
2.7	15	2.0	11.7	4.0	25.0	2.7	11.6	1.2	12.3	3.2
l_5	w_6	l_6	w_s	l_s	w_l	l_l	cw_1	cs_1	cl_1	
25.1	2.7	11.6	2.4	25.4	1.9	25.6	2.6	0.6	12.5	

S_{21} (S_{31}) are -4.754 dB (-1.769 dB), while the measured values of S_{21} (S_{31}) are -4.60 dB (-3.30 dB). The measured value of S_{31} is lower than the calculated value and there is a little frequency shift of S_{11} in Figure 11(b). The difference between the calculated and measured results may be caused by approximate physical dimensions of the microstrip lines, loss characteristic of the F4B substrate, etc.. It can also be observed that the phase difference between the port 2 and the port 3 is $-180°$ in the calculated curve and $-185.24°$ in the measured curve. The phase difference shows that the circuit is a balun. The measured results verify our design.

Based on the investigation on the proposed circuit, a simple design procedure can be summarized as follows.

1) Determine the center frequency f_0, the source and the load impedance (R_s and R_L) according to the design requirements. Choose the values of dielectric constant and thickness of the substrate material.
2) Determine the function of the proposed circuit structure: balun ($0° < \theta_0 < 90°$) or power divider ($90° < \theta_0 < 180°$).
3) Choose the appropriate power division K ($K > 0$). The impedance ration g of the coupled line can be selected to be 1.4. According to Equation (9) and Figure 5, the electrical length θ_0 will be

determined. Use θ_0 and g to calculate the scattering parameters S_{21}, S_{31} at the operating frequency using Equation (9).

4) Use the analytical Equation (1) to determine other unknown parameters Z_i, $(i = 1, \ldots, 6)$. Use the Equations (3), and (5) to determine the values of Z_{e1}, Z_{o1}. Note that all the impedance values are larger than $20\,\Omega$ and less than $120\,\Omega$.
5) Convert all the electrical parameters to the physical dimensions, and simulate the total scattering parameters by using lossless transmission lines. The circuit layout can refer to Figure 9. Note that all the width of the microstrip line are larger than 0.1 mm.
6) Tune the physical dimensions including w_i, l_i, $(i = 1, \ldots, 6)$, cw_1, cs_1, cl_1 to obtain the correct scattering parameters S_{21}, S_{31} and phase difference between the output ports 2 and 3. If other power division K is needed, just tune the value of cl_1 to obtain the appropriate scattering parameters S_{21}, S_{31} and phase difference.

To demonstrate the advantage of this proposed circuit, the comparison is illustrated in the Table 6.

Table 6. The comparison of this proposed circuits with others.

	Methods	Planar Structure	Analytical Design Methods	Arbitrary Power Division	Arbitrary impedance transforming
[3]	Conventional Wilkinson PD	Yes	Yes	No	No
[4–8]	Defected ground structure (DGS)	No	No	No	No
[9–11]	Double-Sided Parallel-Strip Lines (DSPSL)	No	No	No	No
[12]	Composite Right/Left-Handed Transmission Lines (CRLH TL)	No	No	No	No
[13, 14]	Composite Right/Left-Handed Transmission Lines (CRLH TL)	Yes	No	No	No
[15, 16]	A two-port filtering structure connected to a circulator	No	Yes	Yes	No
[17]	Conventional Wilkinson PD with Shunt-stub	Yes	Yes	Yes	No
[18]	Conventional Wilkinson PD with a coupled-line section with two shorts	Yes	Yes	No	No
[19]	Conventional Wilkinson PD with a periodic shunt open stub	Yes	Yes	No	No
This paper	Two branch line coupler and a phase shifter	Yes	Yes	Yes	Yes

5. CONCLUSIONS

A novel four-port circuit structure for implementing PD or balun with variable power division is proposed in this paper. The achieved design approach is analytical and simple. This circuit, constructed by two different couplers and a phase shifter, maintains good return loss, perfect isolation, and arbitrary power division, simultaneously. To demonstrate the practical performance, a microstrip balun is designed, fabricated, and measured. The measured return loss, isolation, the output amplitude and phase difference are good, which verifies the proposed concept for this coupled-line balun. Due to its simple circuit structure and ease of fabrication in common microstrip systems, we believe that this proposed circuit is practical to use and popular in the RF systems.

ACKNOWLEDGMENT

This work was supported in part by National Key Basic Research Program of China (973 Program) (No. 2014CB339900), National Science and Technology Major Project (No. 2012ZX03001001-002), National Natural Science Foundation of China for the Major Equipment Development (No. 61327806), National Natural Science Foundation of China (No. 61201027), Open Project of the State Key Laboratory of Millimeter Waves (Grant No. K201316), and Specialized Research Fund for the Doctor Program of Higher Education (No. 20120005120006).

REFERENCES

1. Wilkinson, E., "An N-way hybrid power divider," *IRE Trans. Microw. Theory Tech.*, Vol. 8, No. 1, 116–118, Jan. 1960.
2. Gysel, U., "A new N-way power divider/combiner suitable for high power applications," *IEEE MTT-S Int. Microw. Symp. Dig.*, 116–118, 1975.
3. Ahn, H.-R., *Asymmetric Passive Components in Microwave Integrated Circuits*, Chapter 6, 156–160, Wiley-Interscience, New Jersey, 2006.
4. Kilic, O. and S. Demir, "Design of a two layer aperture-coupled unequal power divider," *2010 Mediterranean Microwave Symposium (MMS)*, 33–35, 2010.
5. Koo, J.-J., S. Oh, and M.-S. Hwang, "A new DGS unequal power divider," *European Microwave Conference*, 556–559, 2007.
6. Kim, C.-S., J.-S. Park, D. Ahn, and J.-B. Lim, "A novel 1-D periodic defected ground structure for planar circuits," *IEEE Microwave Guide Wave Lett.*, Vol. 10, No. 4, 131–133, Apr. 2000.
7. Lim, J.-S., S.-W. Lee, C.-S. Kim, J.-S. Park, D. Ahn, and S. Nam, "A 4 : 1 unequal Wilkinson power divider," *IEEE Microw. Wireless Compon. Lett.*, Vol. 11, No. 3, 124–126, Mar. 2001.
8. Oh, S., J.-J. Koo, M.-S. Hwang, and C. Park, "An unequal Wilkinson power divider with variable dividing ratio," *IEEE/MTT-S International Microwave Symposium, HI 2007*, 411–414, Honolulu, 2007.
9. Fan, F.-F. and Z.-H. Yan, "Out-of-phase unequal power divider based on parallel dual-lines structure," *2012 International Conference on Microwave and Millimeter Wave Technology (ICMMT)*, 1–3, Shenzhen, 2012.
10. Chen, J.-X., Z.-H. Bao, L.-H. Zhou, and H. Tang, "Novel equal and unequal power divider using offset parallel-strip lines," *2010 International Conference on Microwave and Millimeter Wave Technology (ICMMT)*, 1308–1311, Chengdu, 2010.
11. Chen, J. X. and Q. Xue, "Novel 5 : 1 unequal Wilkinson power divider using offset double-sided parallel-strip lines," *IEEE Microw. Wireless Compon. Lett.*, Vol. 17, No. 3, 175–177, Mar. 2007.
12. Bemani, M. and S. Nikmehr, "Nonradiating arbitrary dual-band equal and unequal 1 : 4 series power dividers based on CRLH-TL structures," *IEEE Transactions on Industrial Electronics*, Vol. 61, No. 3, 1223–1234, Mar. 2014.
13. Zhao, S. W., Z. X. Tang, Y. W. Wu, and B. Zhang, "An unequal broadband power divider using composite right/left-handed transmission lines," *2010 IEEE International Conference on Ultra-Wideband (ICUWB)*, Vol. 2, 1–3, Nanjing, 2010.
14. Liu, C.-J., K.-M. Huang, and W. Menzel, "An unequal power divider using composite right/left-handed transmission line couplers," *IEEE MTT-S International Microwave Workshop Series on Art of Miniaturizing RF and Microwave Passive Components, IMWS 2008*, 216–219, Chengdu, 2008.
15. Zhang, Q. F. and C. Christophe, "Power divider with arbitrary power ratio and arbitrary ripple level using filter synthesis techniques," *Microwave Opt. Technol. Lett.*, Vol. 55, No. 8, 1819–1820, 2013.
16. Zhang, Q. F. and C. Christophe, "Erratum: Power divider with arbitrary power ratio and arbitrary ripple level using filter synthesis techniques," *Microwave Opt. Technol. Lett.*, Vol. 55, No. 10, 2524, 2013.

17. Zhu, Y.-Z., W.-H. Zhu, X.-J. Zhang, M. Jiang, and G.-Y. Fang, "Shunt-stub Wilkinson power divider for unequal distribution ratio," *IEEE Trans. Antennas Propag.*, Vol. 4, No. 3, 334–341, 2010.
18. Li, B., X.-D. Wu, and W. Wu, "A 10 : 1 unequal Wilkinson power divider using coupled lines with two shorts," *IEEE Microw. Wireless Compon. Lett.*, Vol. 19, No. 12, 789–791, Dec. 2009.
19. Kang, M.-S., Y. Kim, and Y.-C. Yoon, "An unequal Wilkinson power divider with a high dividing ratio," *2012 7th European Microwave Integrated Circuits Conference (EuMIC)*, 747–749, 2012.
20. Reed, J. and G. J. Wheeler, "A method of analysis of symmetrical four port networks," *IRE Trans. Microw. Theory Tech.*, Vol. 4, No. 4, 246–252, Oct. 1956.
21. Schiffman, B. M., "A new class of broad-band microwave 90-degree phase shifters," *IRE Trans. Microw. Theory Tech.*, Vol. 6, No. 2, 232–237, Apr. 1958.